190

F.R.I. 47

VERSLAG NR. Physics — magnetic recovery. Fluidized bed combustion. Gen Hydraulics

REPORT NO. 8

VAN

OF 1971

WU1/C4/12

BRANDSTOFNAVORSINGSINSTITUUT
VAN SUID-AFRIKA

FUEL RESEARCH INSTITUTE
OF SOUTH AFRICA

ONDERWERP:
SUBJECT: THE DRAG COEFFICIENT OF A PARTICLE AND THE VOIDS FRACTION IN A FLUIDIZATION OR SEDIMENTATION ASSEMBLY OF PARTICLES.

AFDELING:
DIVISION:

NAAM VAN AMPTENAAR:
NAME OF OFFICER: A.C. BONAPACE.

Cosmi 2074 B 4

INDEX

FUEL RESEARCH INSTITUTE OF SOUTH AFRICA

REPORT NO. 8 OF 1971

THE DRAG COEFFICIENT OF A PARTICLE AND THE VOIDS FRACTION IN A FLUIDIZATION OR SEDIMENTATION ASSEMBLY OF PARTICLES

by

A. C. BONAPACE

1. SCOPE OF THE RESEARCH

Fluidization and sedimentation are basic features of the hydraulics of solid-fluid suspensions.

They form the basis of important industrial processes but for best results conditions have to be closely controlled. In other processes, employing suspensions, these characteristics can create problems if certain facts are overlooked.

It is, therefore, clearly desirable to obtain as much information as possible on the theoretical aspects of fluidization and sedimentation to ensure optimum usage or to avoid pitfalls.

When approaching the subject with this object in view, it appeared that a unified theory might be developed on the basis that, fundamentally, the basic mechanism of fluidization as well as sedimentation is a relative vertical motion between the fluid and the loose assembly of solid particles.

Considered on this basis, a process whereby the assembly of particles is quasi-stationary (relative to the walls of the containing vessel) while the fluid moves vertically upwards would be designated "fluidization". The alternative, where the fluid is stationary and the particles move (downwards) would be designated "sedimentation".

One could also look upon fluidization and sedimentation as a particle transport phenomena albeit, of greatly simplified nature; simple, because the otherwise very complicated phenomenon of flow is here reduced to a high degree of symmetry which greatly facilitates observation.

2. INTRODUCTION

The study of fluidized beds and of particle settling processes in a fluid is ultimately a study of the drag acting on a single particle as an individual of the assembly and of the solids concentration of the bed.

The drag coefficient of a solitary spherical particle when moving relative to a fluid, when rising or falling vertically in a stationary fluid, is a well-known function of the particle Reynolds number.

/The .....

The drag coefficient of a particle in a stream, when transported in low concentrations has been the subject of a previous study[1].

The present investigation is directed at formulating a definition of the drag coefficient of an individual spherical particle in an assembly without imposing any limitation on the solid concentration except for the condition of fluidization.

An assumption is made with regard to the uniformity of the bulk parameters characterizing the assembly, which are regarded, on the average, as constant both in space and time, while each particle is assumed to interact with the surrounding ones only through the shear forces in the fluidizing medium and not by direct contact.

This is a reasonable assumption for the kind of particles considered here, which are of an order of magnitude well exceeding the dimensions of particles undergoing Brownian motion.

Experiments of many authors proved that fluidization and sedimentation can be treated in the same way[2].

In the first process the level of the particle bed is stationary, while the fluid is moving (upwards), in the second process the level of the fluid is stationary and the particles are moving (downwards).

In both cases the velocity is measurable by direct observation, and is defined as fluidization or sedimentation velocity.

The velocity is measured either by observing the fluid flow relative to the stationary level of particles, or by the particle displacement relative to the stationary level of the liquid.

In the first case the flow is always referred to the empty section of the vessel, as if no particles were present, the fluidization velocity V is thus obtained as the quotient

$$V = \frac{Q}{A} \qquad \ldots\ldots\ldots (1)$$

where Q is the volumetric flow rate and A the (empty) cross-sectional area of the containing vessel.

/The .....

The phenomenon of fluidization itself requires a differentiation between "particulate" fluidization and "aggregative" fluidization.

The first term refers to a fluidized solid-liquid system or else a fluidized solid-gaseous system but with limited bed expansion.

The second term refers to fluidized solid-gaseous systems with inherent formation of gas bubbles.

The present analysis deals with particulate fluidization only, and neither considers the cause of the formation of bubbles, nor the effect of bubbles on particles, and vice versa.

3. HYDRAULIC ASPECTS OF THE PROBLEM

Figure 1A, shows a fluidization column of diameter D and cross-section A containing, up to a certain height ho, a mass of spherical particles with diameter d, density ρ_m and initial voids fraction ε_o usually approaching the condition of close packing.

It is assumed that a fluid with dynamic viscosity μ, density ρ, kinematic viscosity $\nu = \frac{\mu}{\rho}$ flows through the column.

The following convention will be used for the velocity symbol: When this is referred to the empty sectional area (no particles obstructing the flow), it has no apex (V), and when referred to a reduced free area (particles present) it bears an apex (V').

Moreover, let the following specific values of V be designated as follows:

Vo : the fluid velocity for conditions of close packing of particles

V_{if} and V_f : the fluid velocities for condition of incipient and general fluidization, with similar designations for volumetric flow rate Q (i.e. Q_o, Q_{if} and Q_f).

Analogously the voids fraction ε is a quantity which varies between a minimum ε_o for conditions of particles in a close packing arrangement (bed height ho) and the value

/ε .....

$\varepsilon = \varepsilon_1 = 1$ when the actual bed height h increases beyond any limit ($h \longrightarrow \infty$) and the upward fluid velocity in the column reaches the limit velocity of the settling solitary particle V_1.

Moreover, a reference system of co-ordinate axes fixed with respect to the walls of the container is introduced:

The voids fraction ε also expresses the percentage-free area of the bed, a well-known fact, which can be proved from geometrical considerations (see Appendix I).

The expression of the interparticle fluid velocity V' is now given separately for turbulent and laminar flow conditions.

V' is made proportional to the free area (ε) for turbulent flow and to the square of the free area (ε^2) for laminar flow.

These assumptions are an extension to the interparticle voids of the laws of flow in conduits.

In symbols:

$$V' = V\varepsilon \qquad \text{(turbulent flow)} \quad \ldots\ldots\ldots \quad (2a)$$

$$V' = V\varepsilon^2 \qquad \text{(laminar flow)} \quad \ldots\ldots\ldots \quad (2b)$$

The body force acting on a particle is the force due to gravity minus buoyancy.

If g denotes the acceleration due to gravity, this force is:

$$F_g = (\rho_m - \rho)g \frac{\pi d^3}{6} \qquad \ldots\ldots\ldots \quad (3)$$

The drag force on a particle is a superficial force which is expressed conveniently as a function of a drag coefficient C_d or C_d' as follows:

For a solitary particle

$$F_d = \tfrac{1}{2} C_d \frac{\pi d^2}{4} \rho V^2 \qquad \ldots\ldots\ldots \quad (4a)$$

For a particle in an assembly

$$F_d' = \tfrac{1}{2} C_d' \frac{\pi d^2}{4} \rho V^2 \qquad \ldots\ldots\ldots \quad (4b)$$

/where .....

where V is the face velocity defined by equation (1).

The ratio between the two drag coefficients, i.e. for a particle in an assembly and for a solitary particle, at equal values of V is:

$$\Phi = \frac{C'_d}{C_d} = \frac{F'_d}{F_d} \qquad \ldots\ldots\ldots (5)$$

The various phases of particulate fluidization can be followed on the diagram of Figure 1B.

For a flow rate $Q<Q_o<AV_o$ the stream moves through a static solid bed of constant voids fraction ε_o (where usually $\varepsilon_o = 0,38$) and constant bed height h_o.

Particles are packed in a certain array with no relative movement.

For a flow rate $Q_o<Q<Q_{if}$ (where $\frac{Q_{if}}{A} = V_{if}$), particles undergo some relative movement but still remain in contact at some points. The voids fraction increases slightly, i.e. $\varepsilon_o < \varepsilon < \varepsilon_{if}$.

For a flow rate $Q = Q_{if}$, one reaches the state of incipient fluidization in which particles have completely lost their physical contact.

At this stage $\varepsilon = \varepsilon_{if}$ is generally of the order of 0,40 for spherical particles. The solid mass is now fully supported by the dynamical action of the flow.

The following analysis deals with spherical particles only.

Experimental results reported in the literature are in agreement with this analysis.

4. DETERMINATION OF THE DRAG COEFFICIENT RATIO Φ

Using definition (3) for the body force due to gravity minus buoyancy and (4a), (4b) for the drag force, the state of dynamic equilibrium on a particle is governed by the equality between body and superficial forces.

Thus for a solitary particle, at equilibrium

$$C_d \frac{\pi d^2}{4} \frac{\rho V^2}{2} = (\rho_m - \rho) g \frac{\pi d^3}{6} \qquad \ldots\ldots\ldots (6a)$$

/and .....

and for a particle in an assembly, at equilibrium

$$C_d' \frac{\pi d^2}{} \frac{\rho V^2}{2} = (\rho_m' - \rho) g \frac{\pi d^3}{6} \quad \ldots\ldots\ldots (6b)$$

where in equation (6b) a new particle density ρ_m' applies.

From equation (6a)

$$C_d = \frac{4}{3} \left(\frac{\rho_m - \rho}{\rho} \frac{g d^3}{\nu^2} \right) \frac{\nu^2}{V^2 d^2} \quad \ldots\ldots\ldots (7)$$

The first bracketed group constitutes the non dimensional Grashof number (Gr), the second is equal to $\frac{1}{Re^2}$, where

$Re = \frac{Vd}{\nu}$ is the Reynolds number.

Thus, under a state of dynamic equilibrium and for a solitary particle

$$C_d = \frac{4}{3} \frac{Gr}{Re^2} \quad \ldots\ldots\ldots (8a)$$

The relation between C_d and Re has been experimentally determined with great accuracy over a wide range of Reynolds numbers (cf. Figure 2 solid line).

For small values (Re< 1), i.e. in the Stokes region, the settling velocity can be determined on the basis of theoretical considerations and follows from the well-known Stokes equation:

$$3 \pi \mu \, dV = (\rho_m - \rho) \frac{\pi d^3}{6}$$

With (6a) this equation yields the following:

$$C_d = \frac{24}{Re} \quad (\text{for } Re < 1) \quad \ldots\ldots\ldots (8b)$$

Equation (8a) may now be used to plot the relation between Re and Gr for the condition of equilibrium as shown graphically in Figure 3 by the curve $\bar{m} = 1$.

In the Stoke region this relation becomes

$$Gr = 18 \, Re \quad (Re < 1) \quad \ldots\ldots\ldots (9)$$

as per direct comparison of Equation (8a) with (8b).

/In .....

In the transition region ($1 < Re < 1000$) and in the turbulent region $Re > 1000$, the curve Gr(Re) can be plotted by using the data of Figure 2.

In a specific case, i.e. in a situation where particle size, density of the medium and of the particle, viscosity are constant, the Grashof number is constant as well. Horizontal lines (i.e. lines of constant Gr number) are thus lines of constant body force, and because of dynamic equilibrium also lines of constant superficial force, while vertical lines (i.e. lines of constant Re number) are also lines of constant velocity.

In the case of an assembly of particles, experimental evidence has shown that equilibrium in an assembly occurs at lower velocities (or Reynolds numbers) than those applying to an identical solitary particle.

In other words equilibrium conditions in the case of an assembly will be found in the zone to the left of the curve $\bar{\phi} = 1$.

As indicated earlier in the case of equilibrium, horizontal lines are lines of constant drag on the individual particle under various conditions of crowding, i.e. for various values of voids fraction ε.

This consideration leads to the concept that the diagram may be extended to illustrate the more general case of equilibrium in an assembly.

Though the actual fluid velocity V' is unknown, the apparent velocity V and the apparent Reynolds number $Re = \frac{Vd}{\nu}$ are available.

Let an isolated particle be at equilibrium at a point P_1, with co-ordinates Re_{P_1}, Gr_{P_1}.

If other identical particles are now introduced into the system, the point of equilibrium shifts to lower velocities or Reynold's numbers along the line $Gr = Gr_{P_1}$ (as the body force or Gr remains constant), say to the point P with co-ordinates

$$Re_{P_2}, \quad Gr_{P_1}.$$

/According .....

According to equation (8a)

$$C'_d = \frac{4}{3} \frac{Gr_{P_1}}{Re'^2}$$

or as

$$Re' = Re_{P_2}$$

$$C'_d = \frac{4}{3} \frac{Gr_{P_1}}{Re_{P_2}}$$

In Equation (5) the factor Φ was defined as the ratio $\frac{C'_d}{Cd}$ at identical face velocities, thus in this case comparison must be made with the drag coefficient at point P_2, i.e. $C_{d_{P_2}}$ as

$$C_{d_{P_2}} = \frac{4}{3} \frac{Gr_{P_2}}{Re^2_{P_2}}$$

and so

$$\Phi = \frac{Gr_{P_1}}{Gr_{P_2}} \qquad \ldots\ldots\ldots (10)$$

One may now plot in the Gr - Re diagram a family of curves Φ = constant (e.g. Φ = 4, 16, 64, etc.). As the diagram is drawn on logarithmic scales, all these curves may be obtained by shifting the basic curve Φ = 1 vertically over a distance corresponding to lg Φ.

A number of points abstracted from experimental data reported by Wilhelm and Kwauk (Ref.3) are inserted in this diagram, the method by means of which the co-ordinates of these points were obtained is indicated in Appendix III.

It is interesting to note that the few points available for non-spherical particles fit satisfactorily into the diagram.

The increase in the drag coefficient as a result of crowding particles together can thus be determined with the aid of the diagram.

/5. .....

5. DETERMINATION OF THE VOIDS FRACTION ε

The line $\Phi = 1$ has been retraced in Figure 4 in the same representation Gr against Re already illustrated in Figure 3.

Let us consider again a point P with projections P_1 and P_2 on the $\Phi = 1$ line.

Then writing as usual V'_p and $Re'_P = \frac{V'_P d}{\nu}$ when describing conditions at point P, one can write according to (8a) and for $Gr = Gr_{P_1}$ = constant.

$$C'_{dP}\, Re'^{2}_{P} = C_{dP_1}\, Re^{2}_{P_1} = Gr_{P_1} \qquad \ldots\ldots\ldots (11)$$

But Re'_p can be expressed in function of Re_{P_1} by means of Equations (2a) or (2b) as follows:

In the case of turbulent flow (a), writing

$$Re'_P = \varepsilon Re_{P_1}$$

and substituting into expression (11) yields

$$\varepsilon = \frac{1}{\Phi^{\frac{1}{2}}} \qquad \ldots\ldots\ldots (12a)$$

In case of laminar flow (b) writing

$$Re'_p = \varepsilon^2 Re_{P_1}$$

and substituting into expression (11) yields

$$\varepsilon = \frac{1}{\Phi^{\frac{1}{4}}} \qquad \ldots\ldots\ldots (12b)$$

Equation (12b) can be further transformed inside the Stokes region because of relationship (8b) into the following:

$$\varepsilon = \frac{Re_{P_2}}{Re_{P_1}}^{\frac{1}{4}} \qquad \text{(for } Re < 1\text{)} \qquad \ldots\ldots\ldots (12b, bis)$$

Loci ε = constant (for values of ε = 0,80, 0,60, and 0,40) have been plotted in Figure 4, by using Equations (11b) and (11b, bis) only, i.e. under the assumption of laminar flow in the inter-particle space.

/The .....

The case of laminar flow is the one most frequently met in practice; it can exist even in cases when the voids fraction is not much smaller than one.

In fact although a solitary particle, if of sufficiently large diameter, will fall according to a turbulent regime, when the concentration of the particles is increased a little, the dimension of the channels between particles becomes small enough to revert the flow to laminar conditions.

Flows through particle beds in turbulent conditions are seldom described in the technical literature.

The only example found in available literature is provided by Kneule F. and Weinspach P.M. (Ref.4) and is described in Appendix IV.

Experimental results from Subba Raju and Venkata Rao (Ref.7) relative to incipient fluidization have been plotted in Figure 4 (details in Appendix III).

The points plotted follow approximately the line $\varepsilon = 0,40$, which can be so interpreted as a locus giving approximate conditions of incipient fluidization.

The graph of Figure 4 is amenable to some interesting considerations. The plane can be divided into three regions: Region I, where the drag exceeds the body forces. Region II, where at various voids fractions dynamic equilibrium is possible for a particle in an assembly of particles. Region III, where hydraulic forces are no longer sufficient to provide conditions of equilibrium and static forces must intervene (friction by contact).

When a point representative of flow conditions approaches from the inside of Region III, its boundary (say the line of incipient fluidization given approximately by $\varepsilon = 0,40$) the granular mass loses its consistency.

A typical case is that of quick-sand which is a fluidized state of the soil produced by a sufficiently high upward velocity of water, generally produced by an underground spring or seepage.

/6. .....

6. APPENDICES

I. The Void Fraction ε as an Expression of the Percentage-Free Area of the Bed

In Figure 5 is shown a certain assembly of spheres forming an elementary cell in a packed arrangement (centres of spheres only are indicated).

The arrangement chosen for the spheres is such that each of them has six adjoining spheres in contact (cubic arrangement).

If ho is the height of the bed in a closely packed state, and N the total number of layers, $\frac{ho}{N}$ is the distance between two contiguous layers of particles.

If by expansion the height of the bed and the distance between previously contiguous layers are doubled to values 2ho and $\frac{2ho}{N}$, respectively, one can assume that some of the spheres (i.e. those with centres surrounded by a small circle) will remain in their old position, while the remainder will move away to a new plane because of the expansion (see Figure 5B).

If $\alpha_o A$ is the original free area and $(1 - \alpha_o)A$ the occupied area, the free area after expansion from ho to 2ho will be $A(\alpha_o + \frac{1 - \alpha_o}{2})$.

By repeating this process for various expansions one obtains the following sequence for:

Free area	Bed height
$\alpha_o A$	ho
$(\alpha_o + \frac{1 - \alpha_o}{2})A$	2ho
$(\alpha_o + \frac{1 - \alpha_o}{2} + \frac{1 - \alpha_o}{4})A$	4ho
---	---
$(\alpha_o + \sum_{p=1}^{n} \frac{1 - \alpha_o}{p^2})A$	2^nho

Then with ε_o and ε_n representing the initial and final voids fractions, respectively, one arrives at the following definition for the voids fraction:

/ε .....

$$\varepsilon_o = \frac{\alpha_o Aho}{Aho} = \alpha_o$$

$$\varepsilon_n = \alpha_o + \sum_{p=1}^{n} \frac{1 - \alpha_o}{2^p}$$

which defines the free area as well.

Moreover

$$\lim_{n \longrightarrow \infty} \varepsilon_n \longrightarrow \varepsilon_1 = 1$$

which is in agreement with what has been previously stated.

II. Information from the Technical Literature. Discussion

The fluidization and sedimentation of solid particles were studied experimentally by R.H. Wilhelm and M. Kwauk[3] with comprehensive tests spreading over the whole range of fluidization - between close packing and full expansion of the bed.

The experimental analysis of these authors was presented in a convenient graphical representation corresponding in practice to a graphical correlation between Grashof and Reynolds numbers of a particle. (See also F. Kneule and P.M. Weinsbach[4]).

Richardson and Zaki[2] particularly studied the expansion of the particle bed for various conditions of fluidization.

P.N. Rowe studied the drag force on a regular array of spherical particles and compared it with the drag force on an isolated particle[5].

L. Davies and J.F. Richardson[6] studied, amongst others, the ratio of the drag force in fluidization, and found them comparable with those of Rowe[5].

K. Subba Raju and C. Rao Venkata investigated the minimum fluidization velocity and inherent condition of porosity for a number of particle sizes, densities, and fluids[7].

In the present work experimental results of Wilhelm and Kwauk, and of Subba Raju and Rao Venkata have been extensively used as a check against the theory developed.

/Some .....

Some hints on the numerical methods followed are provided in Appendix III, so that additional experiments can eventually be discussed in the light of the present theory.

III. Numerical Calculations

The experimental points plotted in Figure 3 are derived from Figure 6, where experiments of Wilhelm and Kwauk covering mainly spherical particles in water have been manipulated as explained hereunder.

Curve No. 3 only deals with the case of a non-spherical particle (i.e. crushed rock); it was used because its Grashof number fits well into the gap between the Grashof numbers of the two contiguous curves.

The construction of the curves of Figure 6 makes use of the concepts which led to Equation (10). Its power of verification lies in the fact that the Reynolds numbers introduced have been experimentally measured on an actual particle bed.

In the light of the theory developed, one can write Equations (8a) and (8b) as follows:

General case $$C'_d = \frac{4}{3} \frac{Gr}{Re^2}$$

Single particle $$C_d = \frac{24}{Re} \varphi$$

where $\varphi = \varphi$ (Re) is a correction factor which outside the Stokes range (Re> 1) takes into account the deviations from Stokes law.

The value of φ can be calculated directly from Figure 2 for any Reynolds number.

Division of previous expressions, member by member, yields:

$$\Phi = \frac{C'_d}{C_d} = \frac{1}{18} \frac{Gr}{Re\varphi}$$

The numerical calculation is carried out for a point Q of curve 1 (Gr = 355), relative to glass spheres with $d = 0{,}29 \times 10^{-3}$ m, close packing voids fraction $\varepsilon_o = 0{,}384$, porosity at Q, $\varepsilon_Q = 0{,}578$, fluidization velocity $V_Q = 6{,}95 \times 10^{-3}$ m/s, these values providing $Re_Q = 2{,}02$ and from Figure 3

$$\varphi(Re_Q) = 1,35$$

Consequently

$$\frac{Gr}{18Re_Q} = 9,75 \text{ and}$$

$$\Phi = \frac{9,75}{1,35} = 7,22, \text{ i.e. point Q.}$$

Figure 7 is just a graphical representation of the tabulated values of Wilhelm and Kwauk.

The experimental points of Figure 4 referred to the work of Subba Raju and Venkata Rao were plotted in a Gr, Re representation by some simple manipulations of the tabulated values, where the Grashof number was expressed by means of the Froude number of a particle in the form

$$\frac{Re^2}{Fr} \frac{\rho_m - \rho}{\rho} = Gr$$

IV. Experimental Verification of Equations (12a) and (12b)

The validity of Equations (12a) and (12b) is checked as follows against experimental results reported in the technical literature.

Voids fraction and velocity are often correlated by various authors in an expression such as:

$$\frac{V}{V_1} = \varepsilon^n \qquad \text{..... (13)}$$

where, in the notation of this work, V_1 is the settling velocity of a solitary particle and V the settling velocity referred to the empty sectional area.

Using Figure 3 regarding the interpretation of points P_1, P_2 and P and their relative Grashof numbers Gr_{P_1} and Gr_{P_2}, one can write the previous expression (13) with the aid of Equation (12a) or (12b) as follows:

$$\left(\frac{Re_{P_2}}{Re_{P_1}}\right)^p = \left(\frac{V_{P_2}}{V_{P_1}}\right)^p = \frac{Gr_{P_2}}{Gr_{P_1}} = \varepsilon_\alpha \qquad \text{..... (14)}$$

/with .....

With

$$n = \frac{q}{p} \qquad \ldots\ldots\ldots (15)$$

The value of q in the context is:

For laminar flow $q = 4$
for turbulent flow $q = 2$

The exponent p is fixed through the slope of the locus $\Phi = 1$ in Figure 3.

For Re> 1000 p is practically equal to 2, as one is in the fully turbulent region.

For Re< 1 p is equal to 1 because the flow is fully laminar (Stokes region).

For $1 < R < 1000$ the values of p are between 1 and 2.

The experimental verification of Equation (12b) is achieved through a comparison of the calculated value of n and those experimentally determined by Richardson and Zaki (Ref.2) in the representation of Figure 8.

These two authors investigated fluidization and sedimentation phenomena in the field $Re < 1000$ and for values of voids fraction low enough to consider the interparticle flow laminar.

Therefore, according to this assumption the value of q in Equation (14) is fixed as $q = 4$.

Some values of $n = \frac{q}{p}$ calculated for particle Reynolds number $Re_{P_1} = 1; 10; 10^2; 10^3; 10^4$ are plotted in Figure 8 as "theoretical points".

The value of $q = 4$ is constant throughout, values of p of the table are calculated from the curve $\Phi = 1$ of Figure 4 by using Equation (14).

The "theoretical" and the experimental points of Richardson and Zaki are in good agreement.

For Re< 1 the experimental points give values of n which are higher than the value of $n = 4$, constant in the region Re< 1.

/For .....

For the verification of Equation (12a) one uses the results of Kneule and Weinspach (Ref.4).

Little information about fluidization and sedimentation at high porosity ($\varepsilon \longrightarrow 1$) and large Reynolds numbers ($Re > 1000$) is found in the technical literature.

The previously mentioned authors, among others, deal with experiments using steel-spheres, the characteristics of which are grouped in the following table.

MATERIAL: STEEL SPHERES: Specific gravity 7,65

Diameter, mm	Settling velocity in water, m/s	Re	Reduction factor, λ
1,5	0,48	720	3,2
3,0	0,80	2 400	1,0
6,0	1,10	6 700	0,36
10,0	1,50	15 000	0,16

The reduction factor λ is here introduced for correlation purposes in order to refer all the Reynolds numbers to a standard one relative to a viscosity of 1 centistokes.

The curve for a kinematic viscosity of 1 centiskes relative to water, appearing in Figure 2 of Kneule and Weinspach's original work, is there plotted in semilogarithmic coordinates as a straight line.

Its equation in the notation used here is the following:

$$e^{(1 - \frac{V_1}{V}\varepsilon)\,0,57} = \frac{\lambda Re}{\lambda Re_1}$$

At the limit for $V \longrightarrow V_1$, i.e. $Re \longrightarrow Re_1$

one gets

$$(1 - \frac{V_1}{V}\varepsilon) \longrightarrow 0$$

that is

$$\varepsilon = \frac{V}{V_1}$$

/This .....

This relationship corresponds to equation (14) written for condition of the turbulent region, i.e. for $Re_1 > 1000$ and for a voids fraction ε high enough to ensure a turbulent inter-particle flow.

Consequently in this case $q = 2$ and $p = 2$, $n = 1$.

7. EXAMPLES OF THE "APPLICATION OF THE THEORY"

i) The Stability of Earth Wall Structures

As is well known the stability of structures such as earth walls of dams, embankments of rivers, etc. is conditioned by the stability of the layer of soil forming the foundations.

Earth walls are structures made of a rather impermeable mass of packed soil, often heaped up against a central core of crushed rock.

Their foundations may consist of a soil of rather porous nature, like alluvial sand or gravel.

Whenever the water percolating through the coarse material of the bed reaches a velocity rate high enough to cause incipient fluidization of the grains, the mass of soil loses its consistency, and the material is carried away by an onrush of water.

This phenomenon called "piping" occurs mostly at the foot of the embankment, on its downstream side (see Figure 9).

Conditions critical for "piping" formation can be established as follows:

The flow through packed beds has been studied by many authors, and particularly by Kozeny, Carman, Burke, and Plummer.

The results of these studies are summarized in the diagram of Figure 10 (Ref.8).

Kozeny, Carman's equation is valid for laminar flow, and can be written as follows:

$$\frac{\Delta P}{\rho_V 2} \frac{d}{L} \frac{\varepsilon^3}{1 - \varepsilon} = \frac{150}{\frac{Re}{1 - \varepsilon}} \qquad \text{..... (16)}$$

where, in addition to the already defined symbols, ΔP is the pressure acting on the bed in the direction of the flow, L is the

/bed .....

bed thickness, in our case the width of the base of the embankment (See Figure 9) and ε is the voids fraction of the packed bed.

In the case of alluvial sand, the grain shape is almost spherical, a fact which makes the grain more prone to movement than when of irregular shape.

Let it be assumed that incipient fluidization takes place for a voids fraction critical value $\varepsilon = 0{,}40$.

When the grain size is small enough (i.e. for $Gr < 750$, which for sand corresponds to $d < 0{,}37$ mm), the curve $\varepsilon = 0{,}40$ of Figure 4 can be represented as follows:

$$Gr = 750\ Re \qquad \ldots\ldots\ldots\ (17)$$

Equation (16) can be transformed by

1) multiplying both members of Equation (16) by $(Re)^2$ (in order to eliminate from one of the members the parameter: velocity (V));
2) expressing ΔP as a fraction of the water height h, i.e. writing

$$\Delta P = \rho g h \qquad \ldots\ldots\ldots\ (18)$$

and

3) introducing in Equation (16) Gr instead of Re (using Equation (17)), to yield finally:

$$tg\alpha_c = i_c = \frac{h}{L} = 0{,}200\ \frac{\rho_m - \rho}{\rho}\ \frac{(1-\varepsilon)^2}{\varepsilon^3} \qquad \ldots\ldots\ (19)$$

This very simple equation yields the stability conditions against "piping" for a foundation made of soil of fine texture ($Gr < 750$).

The critical slope i_c is now completely independent of the particle size, d.

In the case of sand, where $\rho_m = 2600\ \frac{kg}{m^3}$, $\rho = 1000\ \frac{kg}{m^3}$ and $\varepsilon = 0{,}40$ one gets:

$$i_c = 1{,}80 \qquad \text{(valid for } d < 0{,}37 \text{ mm)}$$

/ii) .....

ii) The Stability of a Foundation Soil Made of Gravel with d = 5 mm

The corresponding Gr number is

$$Gr = \frac{gd^3}{\nu^2} \frac{\rho_m - \rho}{\rho} = \frac{9,8 \times 5^3 \times 10^{-9}}{10^{-12}} \times 1,60$$

$$= 1960 \times 10^3$$

From Figure 4, for $Gr = 1960 \times 10^3$, one can establish from the curve for $\varepsilon = 0,40$:

$$Re = \frac{Vd}{\nu} = 330, \quad \text{i.e.}$$

$$V = 330 \frac{\nu}{d} = 0,65 \text{ m/s}$$

$$\frac{Re}{1 - \varepsilon} = \frac{330}{0,60} = 550$$

Then from Figure 10 for $\frac{Re}{1 - \varepsilon} = 550$

$$\frac{\Delta P}{\rho V^2} \frac{d}{L} \frac{\varepsilon^3}{(1 - \varepsilon)} = \frac{h}{L} \frac{gd}{V^2} \left(\frac{\varepsilon^3}{1 - \varepsilon}\right) = 2$$

and finally

$$tg\alpha_c = i_c = \frac{h}{L} = 1,12$$

9. CONCLUSIONS

The fundamental parameters characterizing an assembly of spherical particles in a fluid are the drag coefficient on a particle as a part of an assembly and the voids fraction.

These two parameters have been described in a representation using the Reynolds and the Grashof number of the particle.

In the definition of the Reynolds number, the fluid velocity introduced was that referred to the empty cross-sectional area of the vessel, i.e. defined by the flow rate divided by this area.

The drag coefficient on a particle when in the assembly was expressed as a ratio with the drag coefficient of a settling solitary particle.

/Curves .....

Curves of constant ratio have been graphically produced in a Grashof Reynolds representation by shifting the base curve representing the drag coefficient of a solitary particle towards higher Grashof numbers.

It has also been proved that the voids fraction can be univocally expressed as a function of the drag coefficient ratio.

Two simple functional relationships could be defined: one for laminar, the other for turbulent flow through the bed voids.

The results obtained were checked against experimental results taken from publications in the technical literature and found to be in good agreement with the experiment.

(SIGNED) A.C. BONAPACE
PRINCIPAL RESEARCH OFFICER

PRETORIA.
2nd July, 1971.
/TW

9. NOMENCLATURE, SYMBOLS, AND UNITS

(S.I. units are used)

d	Particle diameter	(m)
g	Acceleration due to gravity	$(m/_s 2)$
h_o	Height of bed in close packing condition	(m)
A	Area of the fluidization vessel	(m^2)
C_d, C'_d	Drag coefficient on a particle for $\varepsilon = 1$ and for $\varepsilon<1$, respectively	
D	Fluidization vessel diameter	(m)
F_g	Force due to gravity on a particle	$(\frac{kg\ m}{s^2})$
F_d, F'_d	Drag force on a solitary particle, on a particle in an assembly, respectively	$(\frac{kg\ m}{s^2})$
Gr	Grashof number $Gr = \frac{d^3 g}{\nu^2} \frac{\rho_m - \rho}{\rho}$	
h	Water level height	(m)
i_c	Critical slope	
L	Length of embankment base	(m)
N	Number of layers of particles	
P	Pressure	$(\frac{kg}{ms^2})$
Q, Q_o, Q_{if}	Flow rate in general, for close packing conditions and for incipient fluidization, respectively	$(\frac{m^3}{s})$
Re, Re'	Reynolds number: $Re = \frac{Vd}{\nu}$ or $\frac{V'd}{\nu}$	
V	Settling of fluidization velocity calculated from the free sectional area A	$(\frac{m}{s})$
V'	Actual fluid velocity (i.e. referred to interparticle free area)	(m/s)

/V_1 .....

V_1	Fluidization or settling velocity relative to a solitary particle	(m/s)
ε_o, ε_{if}, ε	Voids fraction of the packed bed, of the bed at incipient fluidization, of the fluidized bed, respectively; also interparticle percentage free area.	
α_c	Critical angle	
μ	Dynamic viscosity of the fluid	$(\frac{\text{Newton}}{\text{m s}})$
ν	Kinematic viscosity of the fluid	$(\frac{m^2}{s})$
ρ	Density of the fluid	$(\frac{kg}{m^3})$
ρ_m	Density of the material	$(\frac{kg}{m^3})$
Φ	Ratio $\frac{C_d'}{C_d}$	

/10. .....

10. LITERATURE REFERENCES

Ref. 1 Bonapace, A.C., - The Hydraulic Transport of Granular Materials of Uniform Size Composition in Horizontal Pipes.
Coal, Gold and Base Minerals of Southern Africa, August to December, 1968.

Ref. 2 Richardson, J.F., and Zaki, W.N., - Sedimentation and Fluidisation - Part I.
Transaction of the Institution of Chemical Engineers Volume 32 - 1954 p. 35-43.

Ref. 3 Wilhelm, R.H., and Kwauk, M., - Fluidisation of Solid Particles.
Chemical Engineering Progress, vol. 44 No. 3, March, 1948, p. 201-218.

Ref. 4 Kneule, F., and Weinspach, P.M., - Suspendierung fester Koerper in Fluessigkeiten.
Chemie Ingenieur Technik 1963 No. 10, October p. 720-725.

Ref. 5 Rowe, P.N., - Drag Forces in an Hydraulic Model of Fluidised Bed - Part II.
The Chemical Engineer vol. 39 - 1961. April, p. 175-187.

Ref. 6 Davies, L., and Richardson, J.F., - Gas Interchange Between Bubbles and the Continuous Phase in a Fluidized Bed.
Transaction - Institution of Chemical Engineers, Vol. 44, 1966, p. T293-T305.

Ref. 7 Subba Raju, K., and Venkata Rao C., - Critical Mass Velocity in Fluidised Beds.
Indian Journal of Technology, Vol. 2, 1964, p. 222-226.

Ref. 8 Sabri Ergon - Fluid Flow Through Packed Columns.
Chemical Engineering Progress, Vol. 48, February 1952, p. 89-94.

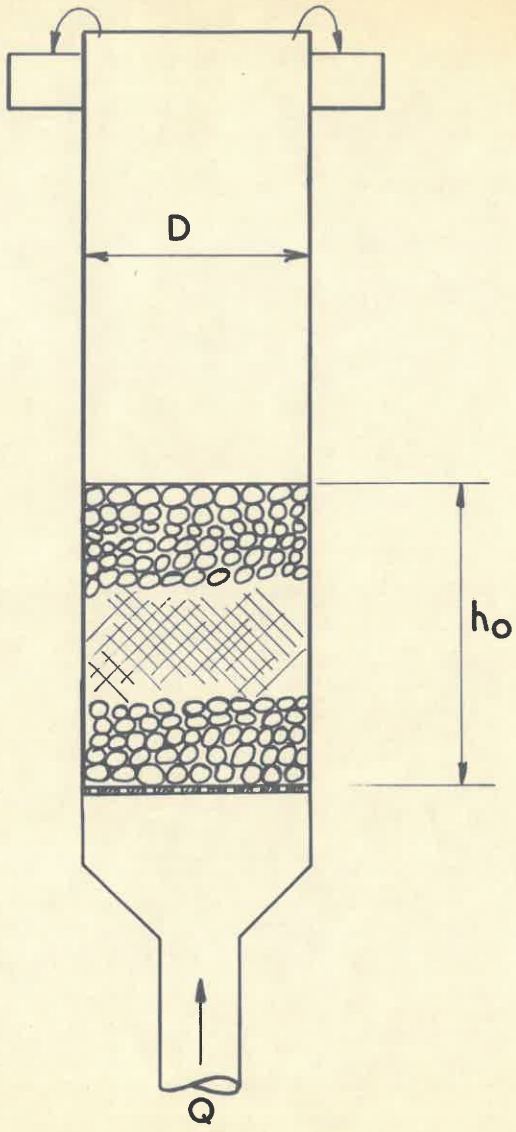

I-A

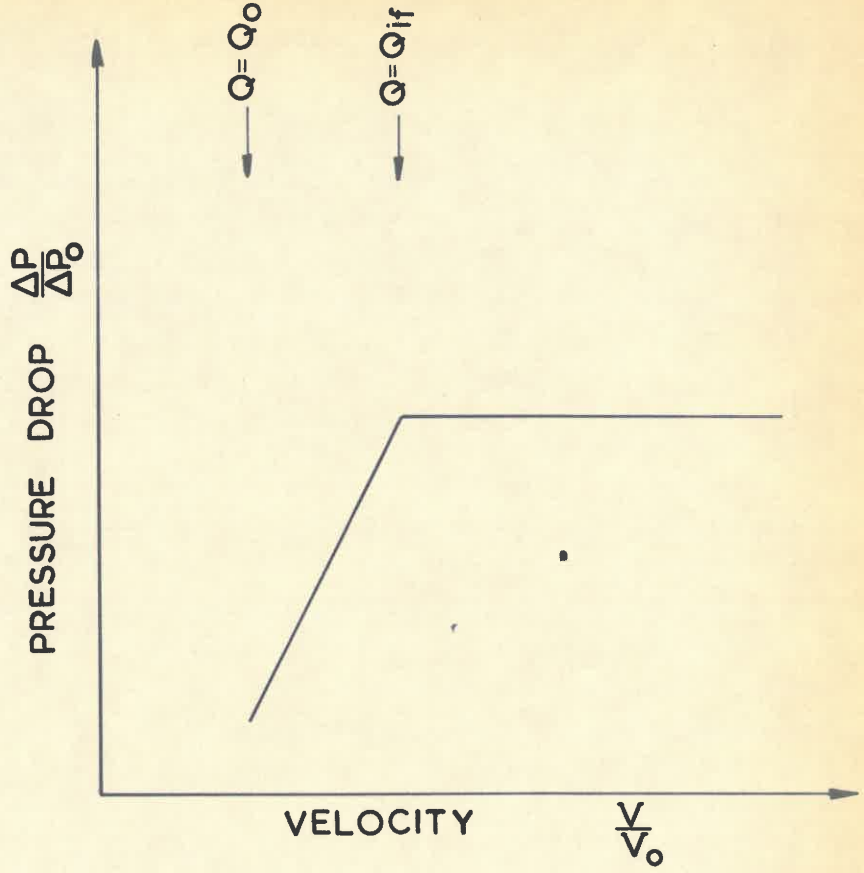

I-B

FLUIDIZATION COLUMN AND FLUIDIZATION DIAGRAM

FIG. 1

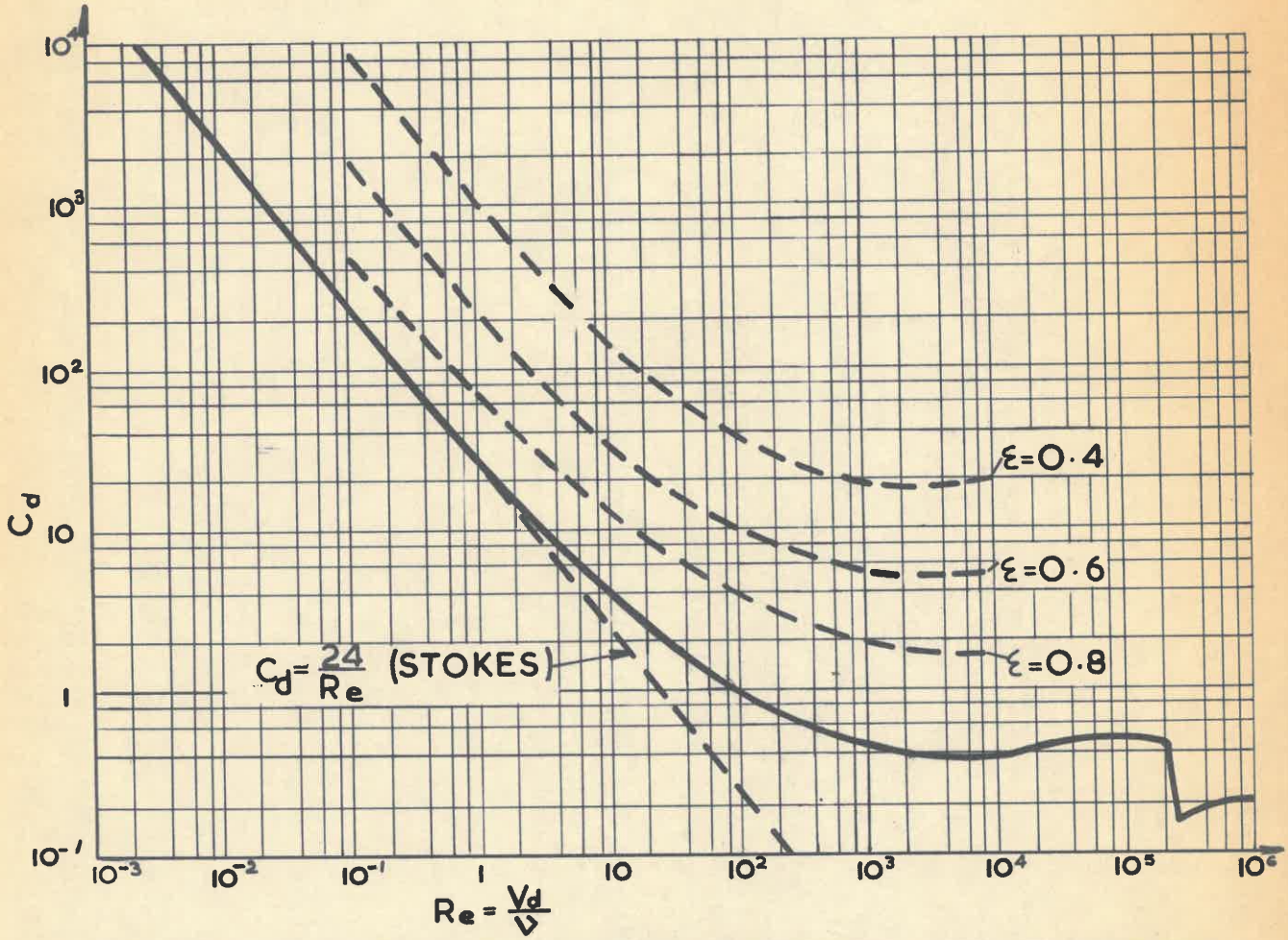

DRAG COEFFICIENT C_d FOR SPHERES AS FUNCTION OF REYNOLDS NUMBER

FIG. 2

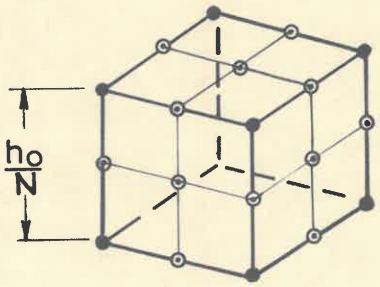

5-A

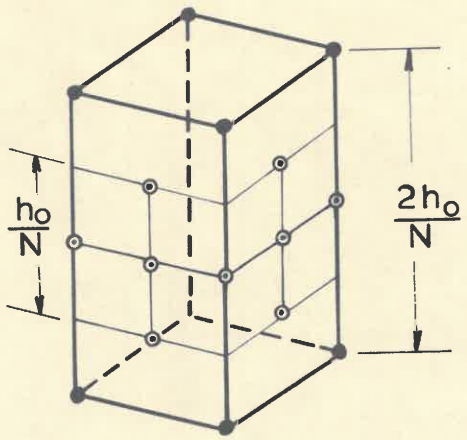

5-B

TWO CONFIGURATIONS OF SPHERES DURING BED EXPANSION

FIG. 5

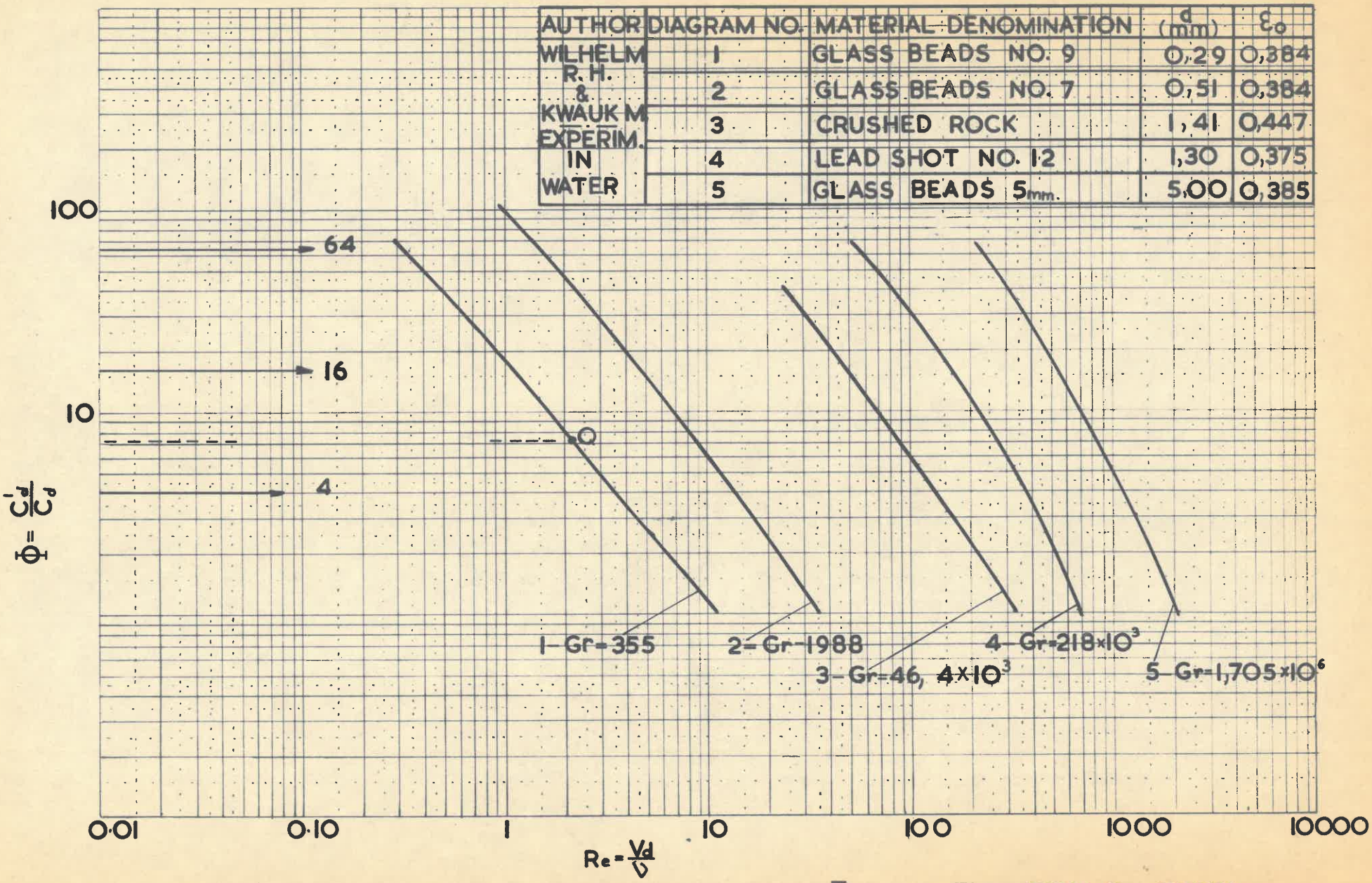

EXPERIMENTAL DRAG COEFFICIENT RATIO Φ AS A FUNCTION OF PARTICLE

FIG. 6

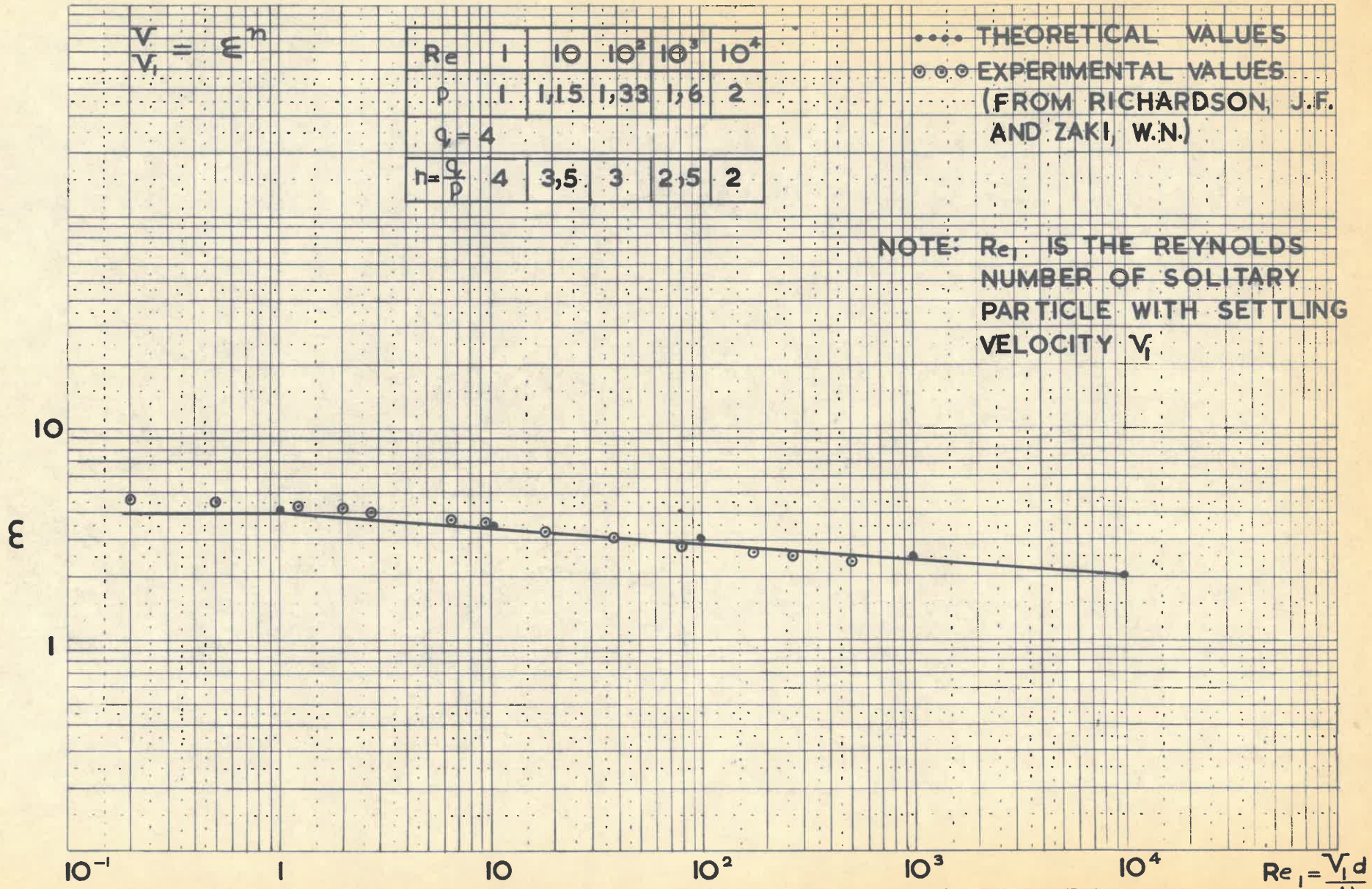

THEORETICAL AND EXPERIMENTAL VALUE OF n AS A FUNCTION OF THE REYNOLDS NUMBER

FIG. 8

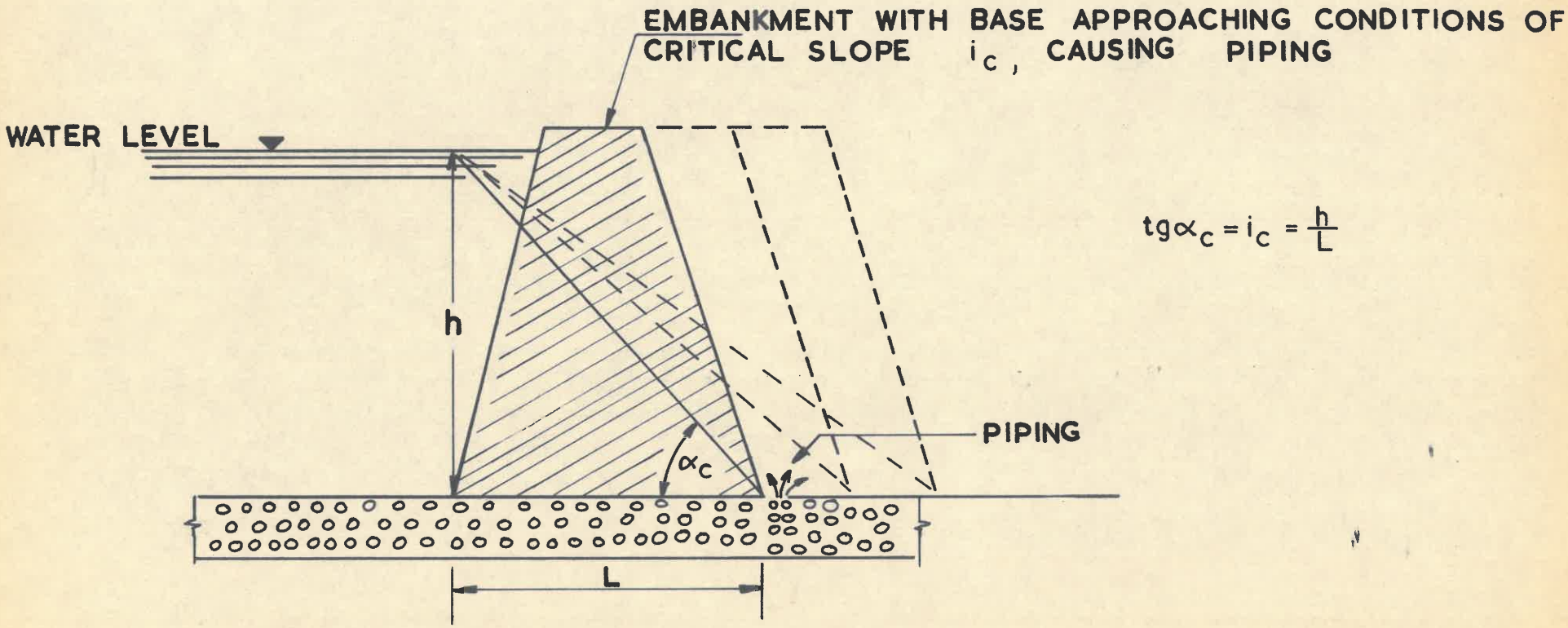

STABILITY OF AN EARTHWALL FOUNDATION

FIG. 9

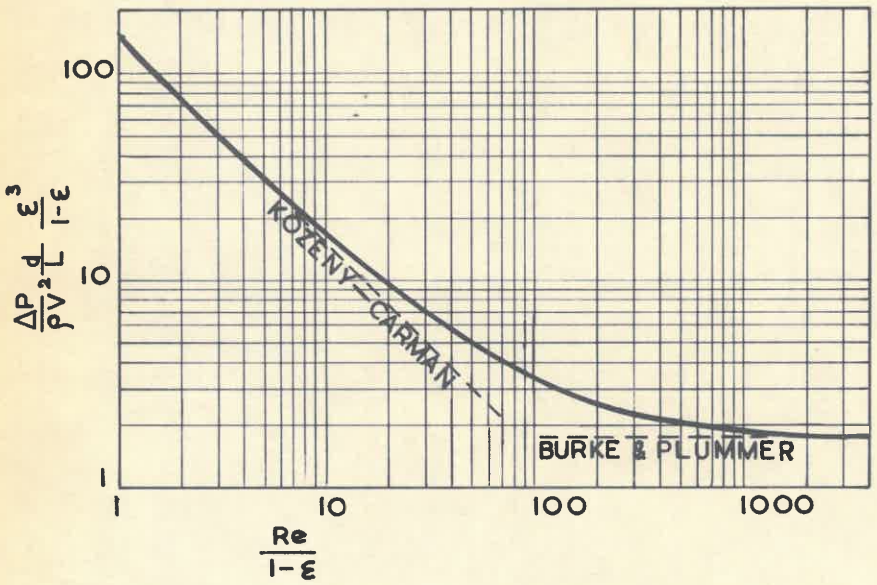

A COMPREHENSIVE PLOT OF PRESSURE DROP IN FIXED BEDS.

FIG. 10

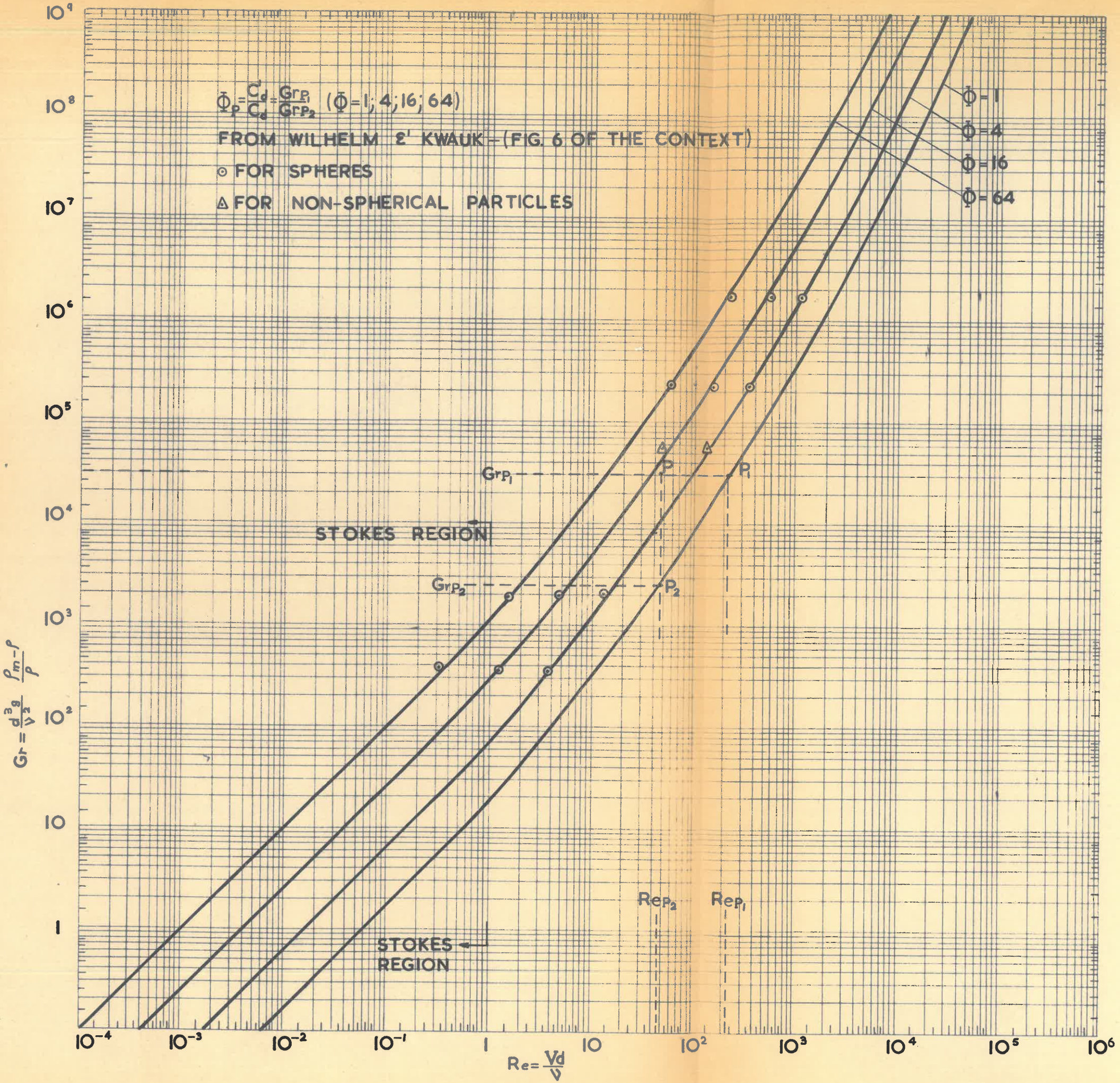

LOCI OF CONSTANT DRAG COEFFICIENT RATIO (Φ) IN A GRASHOF REYNOLDS NUMBERS REPRESENTATION

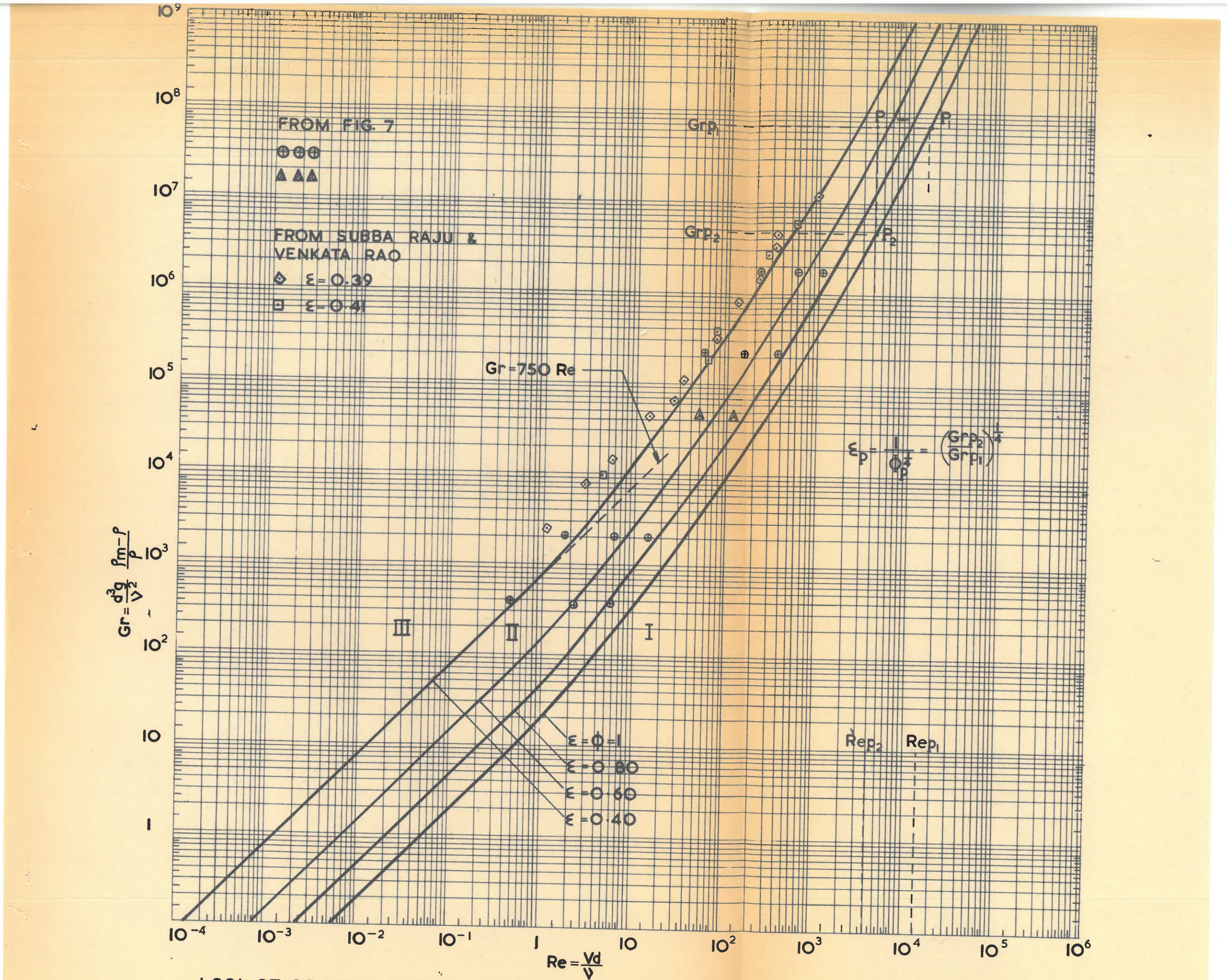

LOCI OF CONSTANT VOIDS FRACTION (ε) IN A GRASHOF REYNOLDS NUMBERS REPRESENTATION

FIG. 4

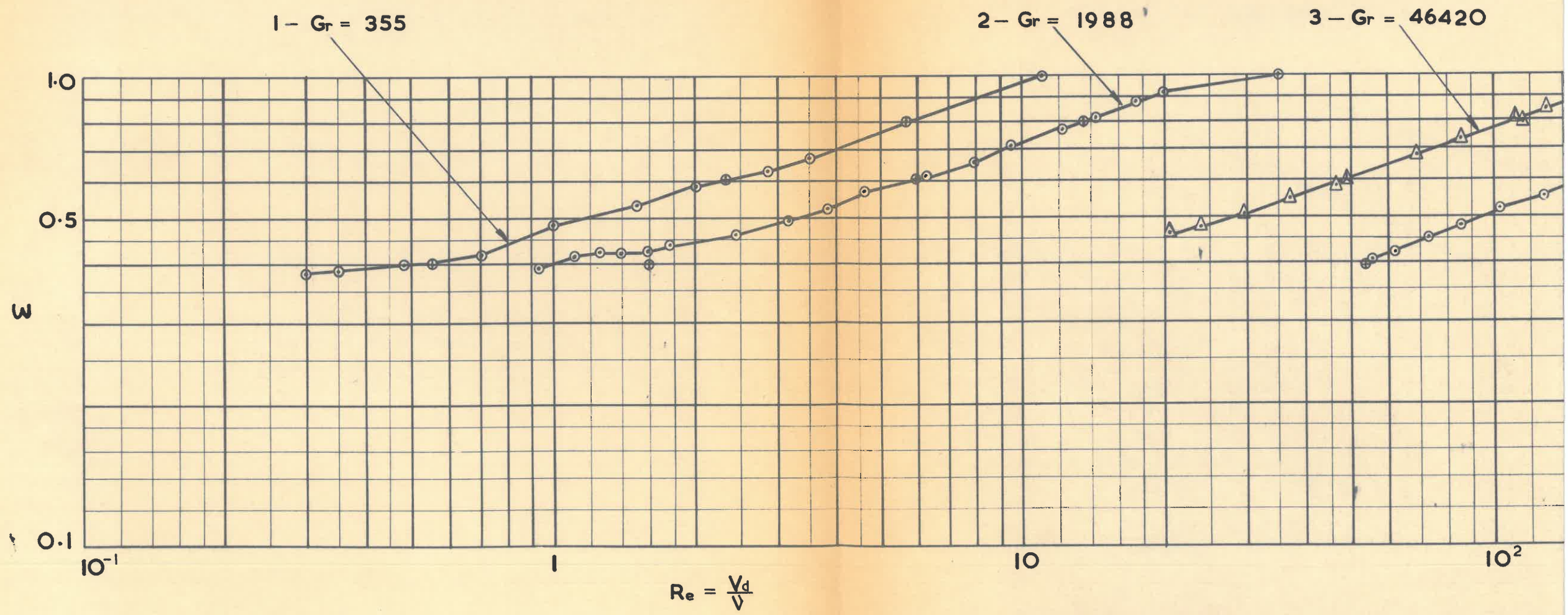

EXPERIMENTAL VOIDS FRACTION ε AS A FUN
REYNOLDS NUMBER (FROM WILHELM R.H.

FIG. 7

⊙ SPHERICAL PARTICLES

△ NON-SPHERICAL PARTICLES

△ ⊕ THESE POINTS DO NOT CORRESPOND TO AN EXPERIMENTAL VALUE, I.E. THESE POINTS ARE EXTRA POLATED.

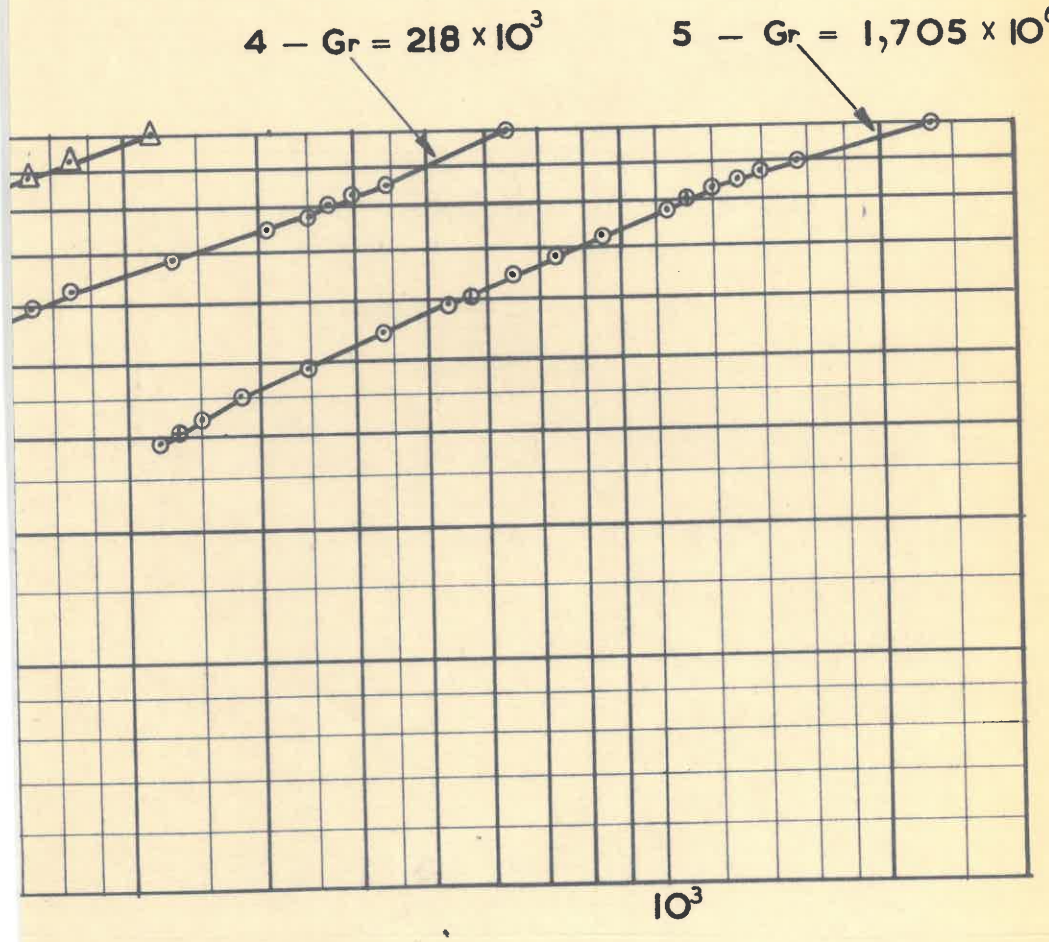

ICTION OF PARTICLE
& KWAUK M.).